NASA-CR-197187

(NASA-CR-197187) INTRODUCTION TO MAGNETIC BEARINGS (USRA) 23 p

N95-12640

Unclas

G3/37 0026165

NASw-4435

IN-37-R
26165
P.23

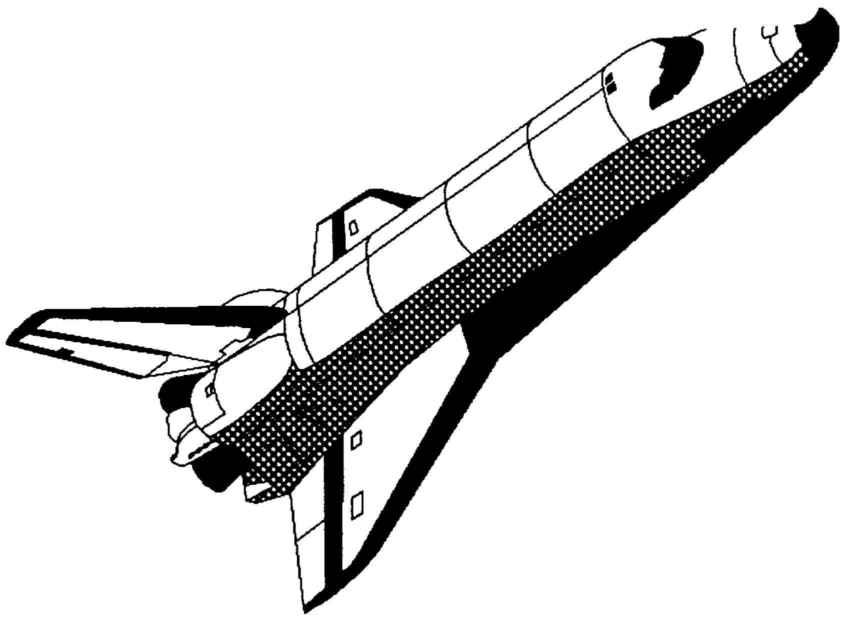

INTRODUCTION TO MAGNETIC BEARINGS

LORI SKOWRONSKI
ANNE BISESE

ECE 485
5 APRIL 1993

INTRODUCTION

Levitation, as far as this report is concerned, is the act of holding up an object with no visible support by means of electromagnetic suspension techniques. Since the 1930's there has been research in single axis suspensions utilizing a magnetic bearing station as shown in Figure 1.

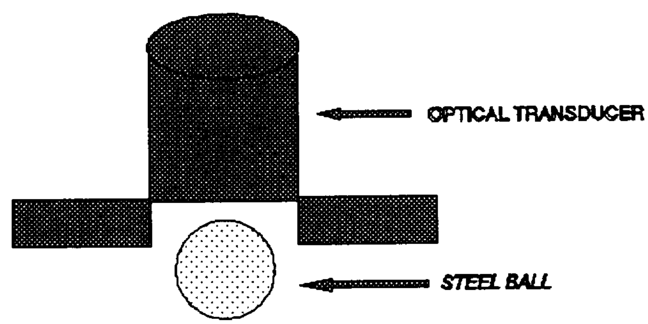

FIGURE 1.

This research has blossomed into the idea of multi-axis suspensions. Multi-axis suspension has several advantages over single axis system, in that it provides control of an object with precision in two or three orthogonal axes. In this report, we discuss the primary use of magnetic-bearing suspension and it's *relevance to what was formally known as NASA's Annular Suspension and Pointing System (ASPS). This system is an experimental pointing system with applications for the space shuttle and the space station programs.*

The objectives behind this magnetic suspension research project are to provide insight to the use of the ASPS configuration, to control the solar panels of the space station. This is important to maintain the correct position of the panels in relation to the sun and orbiting space station for the continuous supply of solar energy. Since the panels are suspended, they can be aligned with minimum outside interference. The approach of using magnetic suspension technology guarantees mechanical isolation since there are no contacting surfaces. This isolation reduces vibration transmission and mechanical wear which in turn extends the life of the payload and of the carrier. It should be noted that ASPS has a high pointing accuracy along the line of 0.01 arc-second.

This research will be done in a laboratory setting by incorporating five bearing stations and one motion control station (See Figure 2). We will attempt to suspend an object of dead weight similar to that of a solar panel. The long term applications may include deep-space navigation, fire control in weapon systems, and an improved mass transit system.

THEORY

The principle behind electromagnetic suspension in this project is simply explained by magnetic flux theory. The magnetic flux through any closed figure is the product of the area by the average component of magnetic induction normal to the area. Flux (Φ) is defined by :

$$\Phi = k \int_s B \, dS$$

where k is the constant of proportionality between field and flux density (B). This application can be expanded to represent the principles surrounding single axis suspension. An object is supported, against the force of gravity, by an electromagnet in which the current is controlled electronically in response to a position signal. From Earnshaw's Theorem, it is known that the stability of the system is dependent upon the feedback of this position signal because without control of the current it is fundamentally unstable. To achieve stable suspension, it is necessary to regulate the current in the electromagnet using position feedback of the object to be suspended.

*The force of attraction between two objects is given by the formula, $F_m = B^2 \div 2\mu_o$ * Area, where B represents the magnetic flux density, μ_o is permeability of free space, and the area is represented by the cross-sectional area of one pole. This formula comes from the derivation of Maxwell's stress formula. The* electromagnets used in suspension systems are under the influence of an "air gap". The air gap denotes a gap left in the magnetic material; a short gap is usually left in the core material to prevent saturation of the magnetic material by the dc current. This implies the gap flux density is directly proportional to the ampere turns "NI" and inversely proportional to the length "g", gap length. The formula then becomes, $F_m = (1/2\mu_o) * (\mu_o * NI/g)^2 *$ Area, as seen by the following derivation.

$$NI = \sum_m H_m l_m$$

where H_m is the magnetic field and l_m is the length of the material.

Maxwell's equation states: $H = \frac{B}{\mu} \quad \therefore \quad NI = \sum_m \frac{B_m}{\mu} l_m$

so, $NI = \frac{B_i}{\mu_i} l_i + \frac{B_a}{\mu_a} l_a$

the first term goes away because $\mu_i \gg \mu_a$

$$\therefore \frac{B_a}{\mu_a} l_a \quad \text{dominates}$$

so, $NI = \frac{B_a}{\mu_a} l_a \qquad \mu_a = \mu_{air} = \mu_o$

for this configuration ------l_a = 2G.W. = g,

substitute into the equation, $B = B_{air}$

$$\therefore \quad NI = \frac{B_{air}}{\mu_o}(g) \qquad \text{solving for } B_a$$

$$B_{air} = \frac{NI\ \mu_o}{g}$$

The governing equation states : $F_m = \frac{B^2}{2\mu_o}$ Area

$$F_m = \frac{[\frac{NI\ \mu_o}{g}]^2\ Area}{2\mu_o}$$

$$F_m = \frac{(NI)^2\ \mu_o^2\ Area}{2g^2\ \mu_o}$$

$$F_m = \frac{(NI)^2\ \mu_o\ Area}{2g^2}$$

However, in this system we have A = 2*(width*length), as with the air gap, taking into account two pole faces.

$$\therefore \quad F_m = \mu_o\ \frac{(NI)^2}{g^2}\ Area$$

The implication of this gap distance is dependent upon several separate factors, the weight of the suspended object, the induced current, and number of turns on the coil. (See Figure 3)

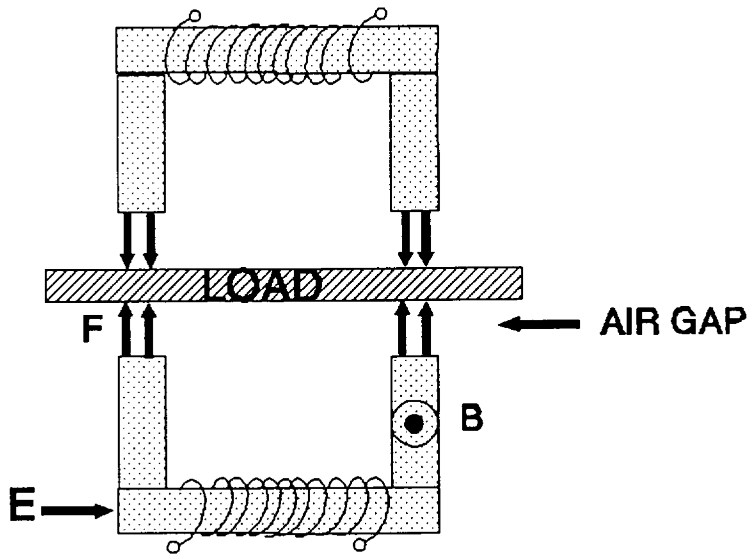

Figure 3

With a

single axis suspension system it is obvious to see that there is only one position on the vertical axis at which the magnetic lift force is equal to the weight of the object. Any deviation to this position will result in the object's displacement.

The translation motion of a free body in space will have three degrees of freedom associated with it as well as three degrees of freedom relating to rotational motion. Again, based upon the classical force equations, the motion equations can be derived for this multi-bearing system. The motion of the system can then be described by six non-linear second order differential equations. The non-lineararity could be due to bearing characteristics and/or rotations due to angular momentum. The equations can be linearized *after utilizing Maxwell's stress formula to find the magnetic stress tensor. The resulting matrix of the tensor provides values for all components of magnetic stress along each of the coordinate axes. The rigid body force acting on an object is obtained by integrating these components over its bounding surface. As far as the rotation due to angular momentum is concerned, a summation of the moments is calculated and then linearized. It should be noted that for efficient operation of suspension systems utilizing dc magnets, small air gaps which can be precisely controlled are required.*

In complicated systems such as the ASPS, multiple bearing stations are utilized. There are several difficulties associated with multi-magnetic systems to include the management of six separate air-gaps. The integrated control portion will be addressed in a separate report.

DESIGN APPROACH

*Using the related force equation, $F = \mu_o \div [(NI)^2 \div g^2]$ *Area, we are to modify the existing multi-bearing system to meet the new requirements assigned. From the design documentation, the weight of the rotor was given as 47.6 lbs or approximately 211.7N. This implies that each bearing station should support 16 lbs or 71.2N. However, to allow for errors and possible addition of payload weight, a 1.3 safety factor is incorporated. Each station should hold 20.63 lbs or a force of 91.75N. An additional factor of 1.5 is included, for control purposes, to give a sum total of 30.94 lbs or 137.63N per axial station. This 1.5 factor is the peak force prior to saturation of the magnetic material. Since the axial magnetic bearing station can hold twice the amount as the radial bearing station, we chose to redesign the axial station first in order to get a reasonable approach to the new requirements. In the formula above, there are five variables that can be changed. Systematically we selected the variable to be altered and made the appropriate calculations.*

In the first design, we regarded the $(NI)^2$ term to be a single factor and the only variable to be considered while all the others were held constant from the original design specifications. This calculation indicated that the "NI" term had to be increased by 54.5% to meet the required specifications. The "NI" term can be broken into it's two components, one involving current and the other number of turns. The number of turns would be very difficult *to increase due to the replacement of the entire coil and the protective coating on the wire. Since it would not be cost effective to increase the number of turns, the alternative is to increase the current. This also is not feasible because increasing the current will cause other problems in the system. These include overheating of the bearings, melting of the wire, and magnetic material saturation. The comparison of the original and new design specifications are shown in Table 1 and Graph 1. The only advantage of this approach would be that the force would increase substantially since* $F \propto (NI)^2$.

In the second design, we regarded the area to be a single factor. To meet the new specifications, the area was calculated to be 1.4E-3 square meters and an increase of 79.3% as shown in Table 1 and Graph 2. We took into consideration an increase in length, width, and a combination of both dimensions. This approach was again not feasible due to cost constraints. It would be very expensive to rebuild the bearing station magnet to meet the new specifications.

The third design took into consideration the gap width. The original specifications set the nominal gap width to be approximately 6.35mm and at the time of this research this was an acceptable distance. Since that time, small-air gap theory, commonly used for magnetic bearing for machinery, has decreased the gap distance to 1/100 of an inch. This new concept led us to the conclusion that the movement of the bearing to decrease the gap width would be the most cost effective and easiest design change.

Taking in to consideration the original design specs and keeping all variables constant, we calculated the gap width to be approximately 3.466mm which is a 83% decrease in distance (see Table 1 and Graph 3). If this decrease should cause saturation or over heating problems, the other design variables will have to be altered. In the testing portion of this report, it is shown that there was no overheating or saturation due to the change in the gap width.

The radial bearing station designs will be minimally modified because the translational motion is negligible. From the original design, we determined that the variables could remain constant with the same change in gap width as the axial bearings.

TABLE 1.

	ORIGINAL	DESIGN	% CHANGE
N--# OF TURNS	2148	4720	+54.5
I--CURRENT	1.4	2.2	+36.4
A--AREA	$2.90X10^{-4}$ m^2	$1.40X10^{-3}$ m^2	+79.3
g--GAP WIDTH	6.35mm	3.47mm	-83.0

Graph 1

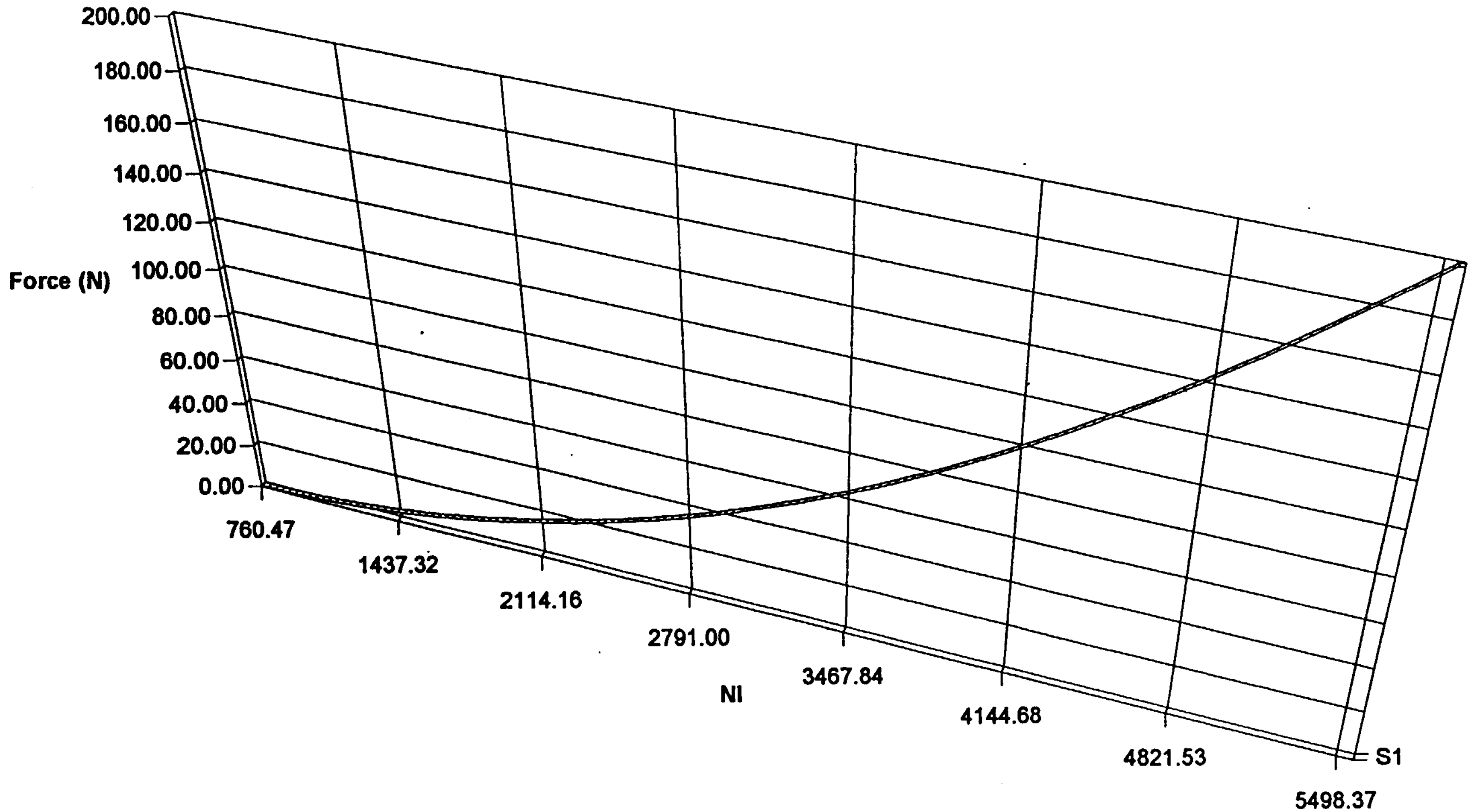

Force (N)
200.00
180.00
160.00
140.00
120.00
100.00
80.00
60.00
40.00
20.00
0.00
760.47
1437.32
2114.16
2791.00
3467.84
4144.68
4821.53
5498.37
NI
S1

Graph 2

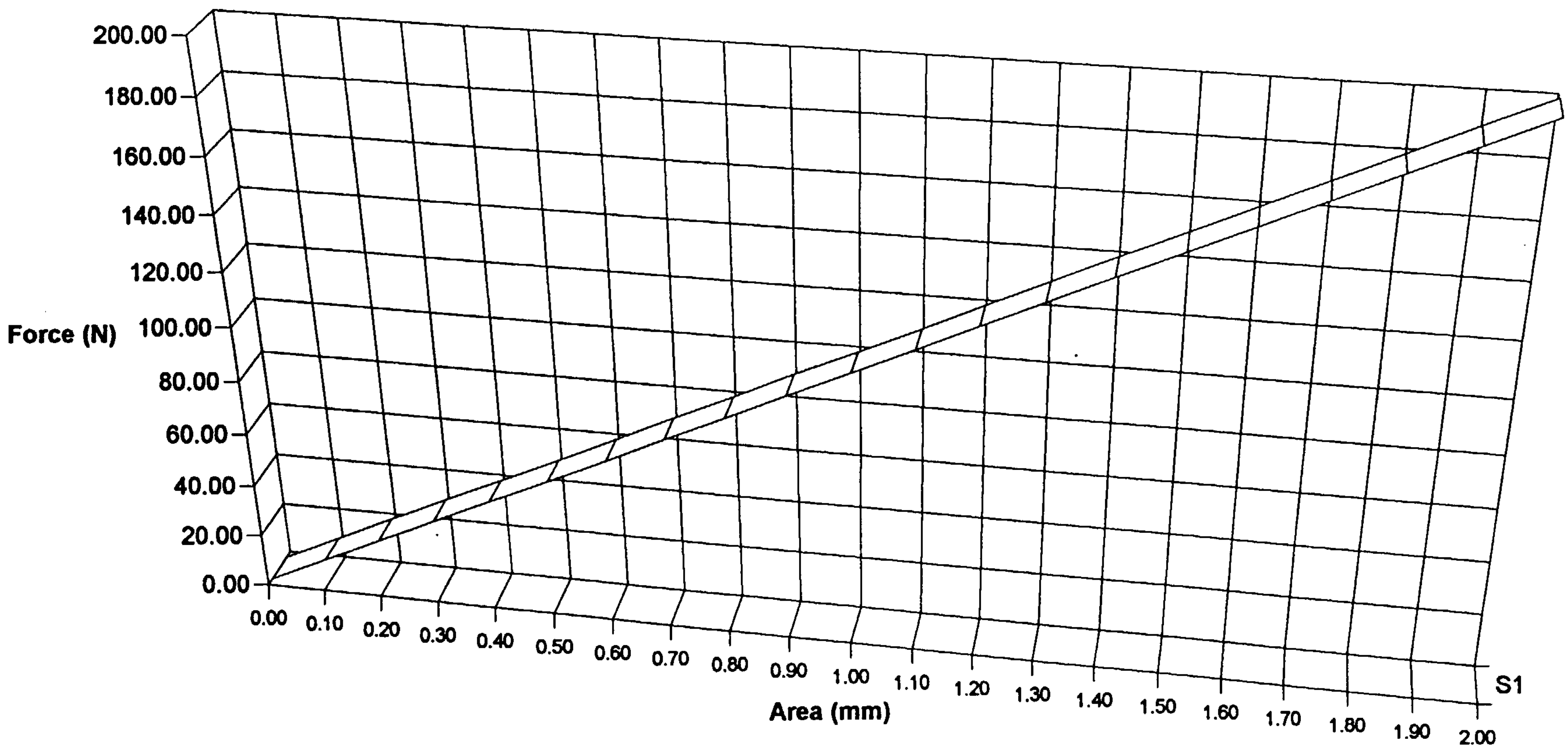

Force (N)
200.00
180.00
160.00
140.00
120.00
100.00
80.00
60.00
40.00
20.00
0.00
0.00
0.10
0.20
0.30
0.40
0.50
0.60
0.70
0.80
0.90
1.00
1.10
1.20
1.30
1.40
1.50
1.60
1.70
1.80
1.90
2.00
Area (mm)
S1

Graph 3

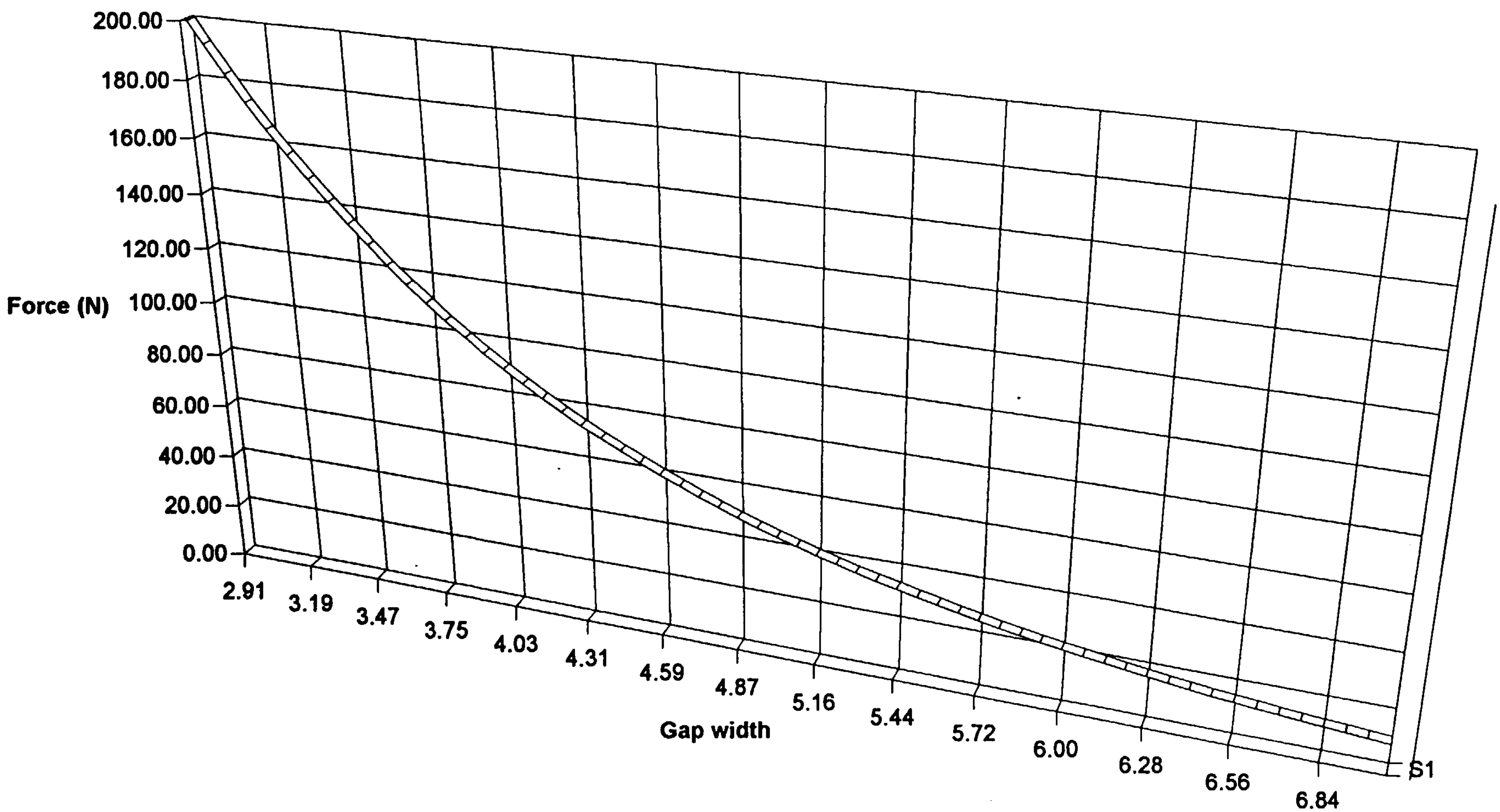
Force (N)
200.00
180.00
160.00
140.00
120.00
100.00
80.00
60.00
40.00
20.00
0.00
2.91
3.19
3.47
3.75
4.03
4.31
4.59
4.87
5.16
5.44
5.72
6.00
6.28
6.56
6.84
Gap width
S1

TESTING AND DESIGN EVALUATION

The original ASPS design and testing was accomplished in the mid 1970's to the early 1980's. Since that time, the ASPS program has been on hold. The purpose of this experimentation is to verify the operational capability of the rotor assembly under new design constraints.

In the new design, the gap width was decreased to increase the lift capabilities. As mentioned in the design section, saturation of the material and overheating of the coils could be two problems encountered by decreasing the gap width. A mathematical exercise can be used to prove the material does not saturate. Knowing that the flux is a constant through out the circuit, flux density in the smallest cross-sectional area can be calculated. The following calculations will show that saturation should not be a problem with the new design.

From previous derivation:

$$B_a = \frac{(NI)\ \mu_o}{2g} = 0.389\ \text{Tesla}$$

$$\Phi = \text{constant} = B_a A_a = B_i A_i$$

$$\therefore\ B_i = \frac{A_a}{A_i} B_a$$

A_i will be the smallest cross-sectional area, which will yield the largest "B"; this will show that saturation does not occur.

$A_a = 1.55E\text{-}3$ $\qquad A_i = 7.76E\text{-}4$ $\qquad B_a = .389T$

$$B_i = \frac{1.55E-3}{7.76E-4}\ (0.389T) = 0.78T$$

As shown in Figure 4, B_{sat} for the material is given as 1.6T. The B_{bias} was calculated as .4T and the "B" for the smallest cross-sectional area is .8T, which is well below the B_{sat} level. There should be no saturation problems due to the new gap width.

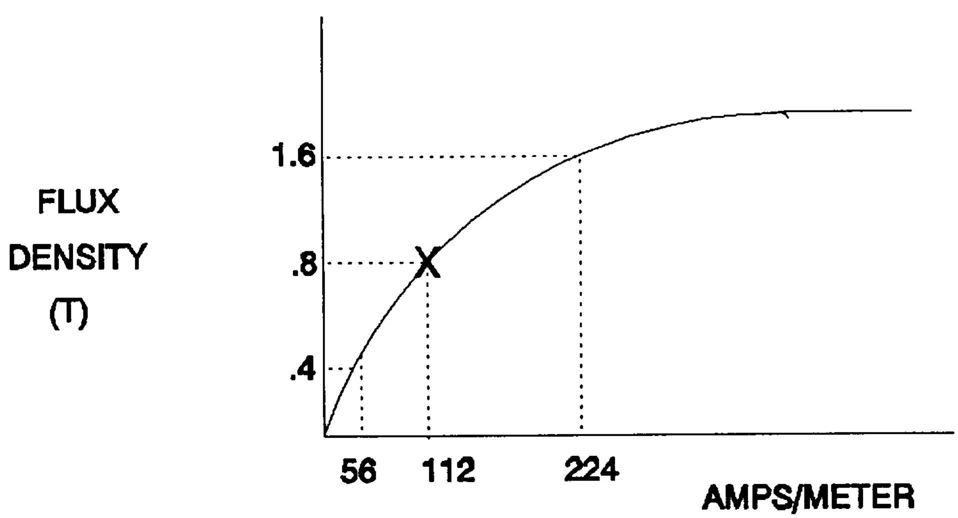

The second consideration mentioned was the overheating of the coils. This was proven in the lab by running a current of 1.5 amps through the coils for twenty minutes. A thermocoupler *was connected to the outside casing of the coil and a piece of foam rubber was positioned around both to insulate them from the outside air. As seen in Graph 4, the increase in temperature was minimal. The current was increased to 2 amps and another twenty minute test of time versus temperature was performed. Graph 5 indicates the increase in temperature was again minimal.*

Each of the bearing stations were tested for their magnetic force by using a 1.5 amp current and a magnetic sensing devise. This proves the magnets are in operating condition.

From these three simple experiments, we believe that our design will function as desired under the specific design criteria.

The actual testing of the rotor assembly was accomplished by the following steps:

1) The schematics indicated the power to the axial bearing stations came from plug J402. Each bearing station is designated by either A, B, or C with pins 1, 9, and 20 being the input and 2, 10, and 21 being the output. To have each bearing station operating simultaneously, the output of A-pin 2 was connected to the input of B-pin 9 and B-pin 10 was connected to C-pin 20. A-pin 1 was connected to the power supply and C-pin 21 was connected to the return.

2) To obtain the appropriate current, two power supplies were connected in series. It should be noted that with them connected in series, the current was monitored by an external amp meter to insure the exact current. We adjusted *the current to approximately 1.6 amps and manually lifted the rotor until it was magnetically held by the top portion of the bearing assembly. We then decreased the current at 0.01 increments until the rotor released itself at approximately 1.35 amps.*

3) The desired air gap was maintained by inserting a non-magnetic material (aluminum) shim to simulate an air gap of 3.46 millimeter. Therefore, when the rotor was raised, the assembly was operating at the designed criteria. The results are shown in the accompanying photographs.

Table of Temperature (C) Increase

Time (Minutes)	0.00	1.00	2.00	3.00	4.00	5.00	6.00	7.00	8.00	9.00	10.00	11.00	12.00	13.00	14.00	15.00	16.00	17.00	18.00	19.00	20.00
Graph 4																					
Actual	23.60	24.20	25.40	26.60	27.80	28.80	29.60	30.60	31.40	32.00	32.80	33.20	34.00	34.40	35.00	35.60	35.60	35.60	37.00	37.00	38.00
Theoretical	23.60	24.39	25.18	25.96	26.75	27.54	28.33	29.12	29.91	30.69	31.48	32.27	33.06	33.85	34.64	35.42	36.21	37.00	37.79	37.79	37.79
Graph 5																					
Actual	23.60	24.40	26.60	29.20	31.60	33.80	35.80	37.60	39.40	41.00	42.80	44.40	45.80	47.20	48.60	49.60	51.00	52.20	53.20	54.00	55.00
Theoretical	23.60	25.34	27.08	28.82	30.56	32.31	34.05	35.79	37.53	39.27	41.01	42.75	44.49	46.24	47.98	49.72	51.46	53.20	54.94	54.94	54.94

Graph 4

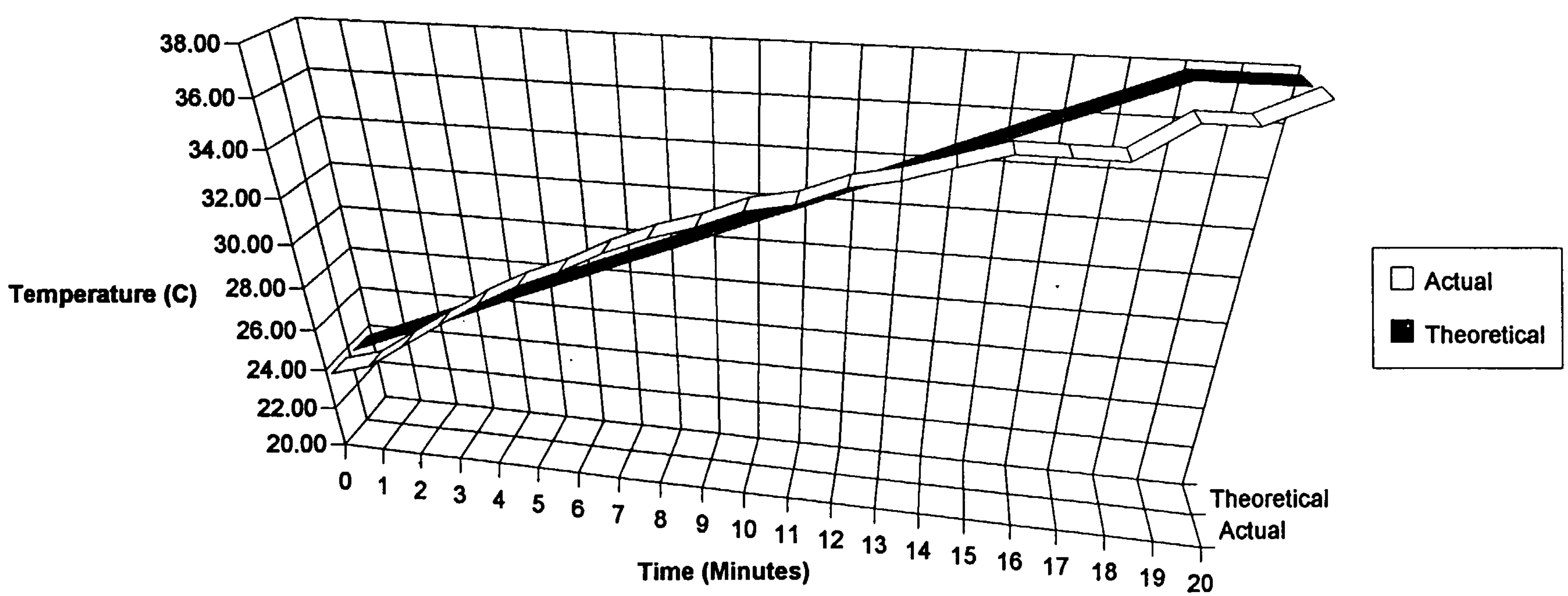

Temperature (C)
38.00
36.00
34.00
32.00
30.00
28.00
26.00
24.00
22.00
20.00
0 1 2 3 4 5 6 7 8 9 10 11 12 13 14 15 16 17 18 19 20
Time (Minutes)
Theoretical
Actual
Actual
Theoretical

Graph 5

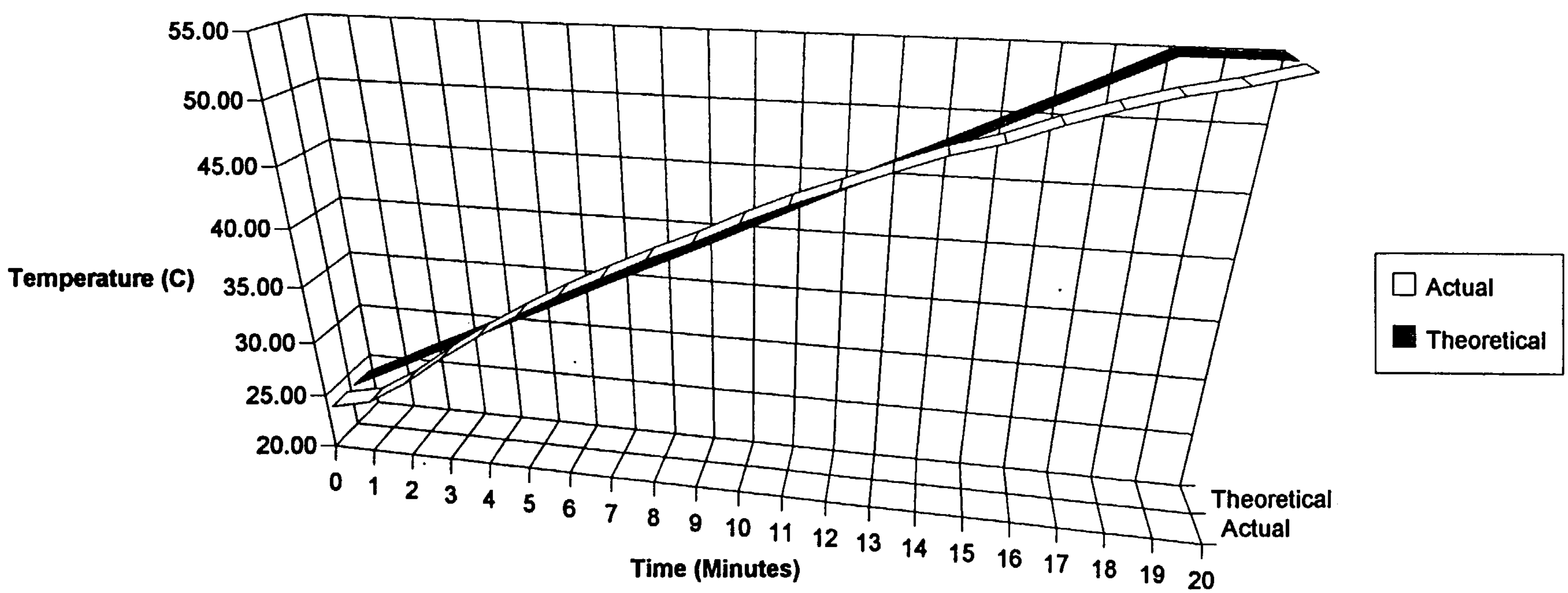
55.00
50.00
45.00
40.00
35.00
30.00
25.00
20.00
Temperature (C)
0
1
2
3
4
5
6
7
8
9
10
11
12
13
14
15
16
17
18
19
20
Time (Minutes)
Theoretical
Actual
Actual
Theoretical

CONCLUSION

Based on the design calculations, the assembly operated within acceptable limits. The current designed for was 1.4 amps, however, the assembly operated correctly at 1.35 amps. This indicates that the assembly could operate at lower currents and also implies there would be no problem with overheating of the coils or saturation of the magnetic material.

The follow-up research for the magnetic bearing system should include integration of the roll-motor assembly with the findings of this report. This would give control of the entire bearing system to roll-motor assembly instead of the few pins referenced in the experimental section of this report. A computer program could be used in conjunction with the control motor for ultimate control of the system.

REFERENCES

1) *International Symposium on Magnetic Suspension Technology, NASA Conference Publication 3152 Part 1.*

2) *B. V. Jayawant, Electromagnetic Levitation and Suspension Techniques.*

3) *Robert R. Humphris, Introduction to Magnetic Bearings*

4) *The Development of the ASPS Vernier System, Final Report, Sperry Corporation.*

5) *ASPS--Final Design Review, Sperry Corporation.*

6) *G. F. Franklin, J. D. Powell, A. Emami-Nasini, Feedback Control of Dynamic Systems.*

7) *F. T. Holmes, Axial Magnetic Suspensions, Physics Review.*

8) *A. T. Carmichael, S. Hinchliffe, P. N. Murgatroyd, I. D. Williams, Magnetic Suspension Systems with Digital Controllers, Review of Scientific Instruments, Aug. 1986.*

9) *M. B. Scudiere, R. A. Willems, G. T. Gillies, Digital Controller For A Magnetic Suspension System, Review of Scientific Instruments, Aug. 1986.*

10) *R. G. Lerner, G. L. Trigg, Encyclopedia of Physics.*

11) *D. M. Considine, Van Nostrand's Scientific Encyclopedia.*

12) *L. Chi Shen, J. Au Kong, Applied Electromagnetism.*